Transient Pressures from Compression of Discrete Air Pockets in Rapidly Filling Combined Sewer Storage Tunnels

Steven J. Wright, Kelley V. Determan, and Silvana D. Vargas

University of Michigan
Civil & Environmental Engineering
Report UMCEE 2010-4
August 2010

1 Background

1.1 Introduction

Numerical simulations of the filling of large diameter combined sewer storage tunnels suggest that the filling process may result in the entrapment of a large discrete air pocket as the tunnel becomes surcharged. The specific process is described in more detail below. Current numerical models do not directly account for the presence of the trapped air in order to reduce model complexity. If the trapped air cannot be readily vented at the entrapment location, the air becomes compressed. The existing numerical modeling frameworks (examples include Cardle and Song, 1988; Politano, et al, 2007; Capart, et al, 1997 and Vasconcelos, et al, 2006 although these models have not necessarily been set up to explicitly model the process of air entrapment) ignore this process and the single phase models instead effectively presume that the air vanishes from the system, resulting in water hammer pressure transients as the two columns of water on either side of the air pocket collide. These transients yield an initial high pressure wave followed by a subsequent low pressure one. It is known that the interaction of a filling flow will also result in qualitatively similar behavior when trapped air is compressed inside a filling pipeline e.g. Martin (1976). It is important to note that water hammer and air compression are two fundamentally different processes. There is no reason to expect the same pressure changes from the two phenomena and, in fact, it is possible that under certain sets of conditions, either process could result in greater pressure variations. The purpose of this experimental study was to measure the pressure transients associated with a filling flow during which a discrete pocket of trapped air is compressed by the water flow. There have apparently been no such experiments performed previously to address this issue.

1.2 Summary of Findings

The challenges of trying to measure the pressure within a trapped air pocket that changes location with the experimental conditions forced some compromises in the experimental design. Experiments were performed by initiating a transient by opening a valve in the closed pipeline adjacent to a constant head reservoir. Initial experiments were performed in a down-sloping pipe such that the air was trapped immediately downstream of the valve. Because the water flow is starting from a stagnant condition, air always flowed back through the valve and into the reservoir leaving an air volume within the pipe that decreased with time. In order to avoid the complications of interpreting those experimental results, the experimental configuration was altered to study two conditions: one in which the air was distributed along the top of an up-sloping pipe so that air could not escape back through the valve and another configuration in which the air was confined within a vertical section downstream of an elbow at the

downstream end of the pipeline. Relatively modest pressure rises were noted in both these configurations, due to the fact that the air compression immediately after opening the valve prevented the water flow from becoming established. These experiments were judged to not be representative of the conditions expected in a rapidly filling tunnel. Nevertheless, several relevant findings were:

- As the trapped air volume became smaller, everything else being the same, the pressure rises increased, but these increases are modest;
- There did not appear to be any significant difference whether the air was distributed along the crown of the pipe as opposed to being confined to the downstream end of the pipe with similar pressure peaks and inertial oscillation periods in both sets of experiments;
- Minimum system pressures were above atmospheric or only slightly below.
- A rigid column analysis specifically developed to simulate the experiments in which the air was trapped in the vertical portion of the pipe beyond the downstream elbow was reasonably successful at predicting the peak pressures observed in those experiments as well as the inertial oscillation periods. One finding that was a bit unexpected but somewhat consistent with observations in related experiments is that the experiments showed a much more pronounced damping of the pressure oscillations than the numerical predictions. Unrealistically high energy loss coefficients would be required to match the decay in the pressure amplitudes, suggesting that some other mechanism may be producing energy losses in these experiments. If the loss coefficient was arbitrarily adjusted to produce a consistent pattern of oscillation decay, then the peak pressures were quite well predicted.

In order to perform more representative experiments, the experimental configuration was revised. A ventilation shaft with a valve located at its base was installed near the downstream end of the pipeline. Experiments were initiated with this valve in the open position so that air could escape from the pipeline; this resulted in the formation of a pipe-filling bore that pushed the air ahead of it and through the ventilation shaft. The valve was rapidly closed to trap an unknown (but measureable) volume of air within the pipe ahead of the advancing bore. Since the water flow had more opportunity to accelerate in this configuration, substantially greater pressures were observed during the compression of the trapped air that remained in the pipeline following valve closure. Findings from this set of experiments were:

- Much higher pressure rises were observed in this set of experiments, even though the reservoir heads were much smaller than the previous experiments; this is attributed to the fact that the experimental setup allowed the hydraulic bore to become well established prior to the air

compression, a situation that is consistent with the air entrapment scenario described further below.

- Again, the smaller the trapped air volume, the greater the initial pressure rise with a more pronounced effect in these experiments;
- In addition, minimum pressures following the rebound of the compressed air behaved in a similar fashion in that more sub-atmospheric pressures (lower minimum absolute pressure) were observed when the initial peak pressure was higher;
- Minimum pressures observed were substantially below atmospheric, which is reasonable to expect since the initial air pressure in the system is atmospheric, the maximum pressure rise on air compression goes above atmospheric and the subsequent pressure drop with the rebound of the compressed air dropping the pressure below the equilibrium state;
- The magnitude of the pressure variations also depended on the strength of the bore which could be controlled by varying both the initial water depth in the pipe or the reservoir head with greater pressure variations associated with stronger bores. The effect of initial depth was much more significant than that of the initial reservoir head;
- Using some heuristic arguments to develop non-dimensional parameters, the experimental data could be collapsed to a simple relationship between pressure maxima and minima and trapped air volume. Experiments performed in a shorter pipe about 60 percent of the length of the original pipe were consistent with the experiments, indicating that the water mass behind the filling bore is not a critical factor in the pressure variations. Some more work will be required to demonstrate the generality of the relationship.

In the near future, the experimental investigation will be supported with numerical simulations using a variation of the Vasconcelos, et al (2006) model to clarify the predictions of modeling with a single phase (water only) model. However, it is clear that the pressure variations observed in the experiments are associated with compression of the trapped air, a phenomenon that is not included in the numerical framework. Since the magnitudes of the observed pressure variations is dependent on the trapped air volume, it is anticipated that pressure rises may be more than predicted by the numerical model if the trapped air volume is sufficiently small and vice versa. We are also investigating the capability of extending the model to at least predict the initial pressure rises by including the compression of trapped air in a fashion similar to outlined by Vasconcelos and Wright (2009). In the meantime it appears as though the dimensionless results presented in Figures 14 and 15 can be extrapolated to prototype conditions but quite extreme pressure variations are predicted. An important question seems to be

whether a strong bore is present at the onset of air pocket compression. The filling scenario described in the following section appears to admit the possibility.

1.3 Tunnel Filling Process

Based on the application of the Two Pressure Component Approach (TPA), a numerical procedure developed by Vasconcelos, et al (2006), to a number of prototype tunnel systems, an understanding has been developed of a fairly common scenario for tunnel filling that results in the entrapment of a discrete pocket of air somewhere along the conduit. This description is generic, but we are aware that many existing and proposed systems have this general geometry and are therefore prone to the sequence of events. Many tunnel systems are constructed with a small slope towards one end to facilitate tunnel emptying and flushing following a rainfall event that results in inflow to the tunnel through a number of dropshafts. Initially, the filling rate is fairly low at the beginning of the runoff process and water tends to accumulate at the low end of the tunnel. Eventually, the system may become full later in the runoff event at a time where the inflow rates may be substantially higher. This may result in a hydraulic bore (moving hydraulic jump) that travels upstream as a filling front. Due to the existence of additional storage in side tunnels or in vertical shafts, the pipe-filling bore may evolve into a standard free surface bore followed by a gradually increasing water depth behind the bore until the free surface touches the tunnel crown (Wright, et al (2008) termed this a *gradual flow regime transition*). When the upstream migrating bore reaches the upstream end of the tunnel or a significant tunnel transition, the bore reflects and begins to migrate towards the low end of the tunnel as a pipe-filling bore. Wright, et al (2008) demonstrated the difference between the pipe filling bore and the gradual flow regime transition and suggested that the gradual flow regime transition could trap significant volumes of air. The air becomes trapped between the downstream propagating bore and the upstream migrating gradual flow regime transition. Figure 1 is a schematic representing the process. Assuming that there is no ventilation provided above the air pocket, the air becomes compressed and will also be transported along the tunnel crown (the direction depending on the interplay between the tunnel slope and the inertia of the bore) until it reaches a ventilation point through which pressure relief may occur. Because the compression process will occur relatively quickly, a significant pressure rise may develop before the ventilation becomes effective and this will be followed be a subsequent pressure drop due to the rebound of the compressed air. Vasconcelos and Wright (2009) demonstrated through simulations and experiments that the compression of air may result in the breakdown of the pipe filling bore and the subsequent intrusion of air against the oncoming bore.

Studies in the past have provided some insights into the effects of air compression on pressures within the water flow. Martin (1976) made simulations for a pipeline with a trapped pocket of air (or a situation in which the air outflow is restricted by an orifice) with a flow initiated by the sudden opening of a valve at the reservoir end of a pipeline. He showed that the volume of air trapped is a key variable with smaller air pockets resulting in higher pressure rises. Zhou, et al (2002) applied a similar analysis as well as conducting experiments involving a sudden inflow of water into a sewer pipeline in which it was assumed that the air was forced out through a restricted ventilation point at the downstream end of the system and showed that quite large pressure rises were possible. The numerical modeling for both these approaches takes a "rigid column" approach in which it is assumed that the sudden inflow creates a vertical front in which the air is forced ahead of the advancing water front. Although the experiments of Zhou, et al did not produce such a vertical filling front, they report good agreement between their experimental and numerical results. However, in order to create the experiments, their choice of setup resulted in flow conditions that are unrealistic for filling sewer systems and in any case, their numerical model cannot be expected to relate to the filling scenario described above. In their visualization of the filling process, it would be a quite straightforward matter to design adequate ventilation at the downstream end of the system. In the scenario that we describe above, the provision of adequate ventilation becomes much more problematic since the air is trapped somewhere along the pipeline at a location that will vary depending on the filling history of the tunnel (although in general, it should be towards the up-slope end of the tunnel) and unless very closely spaced ventilation points are provided, it would be hard to avoid some degree of air compression.

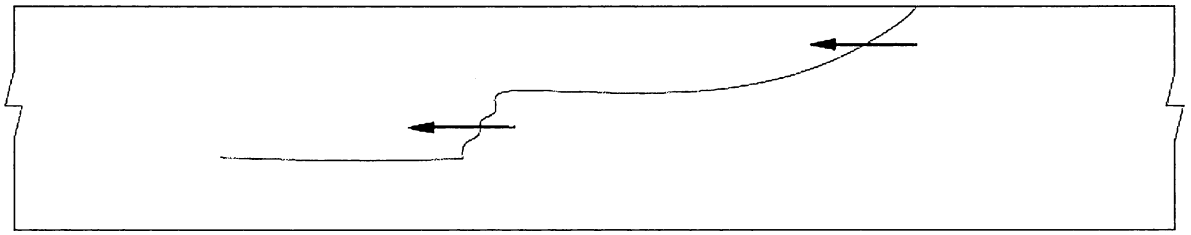

a.) Free surface bore advancing to up-slope end of tunnel followed by gradual flow regime transition.

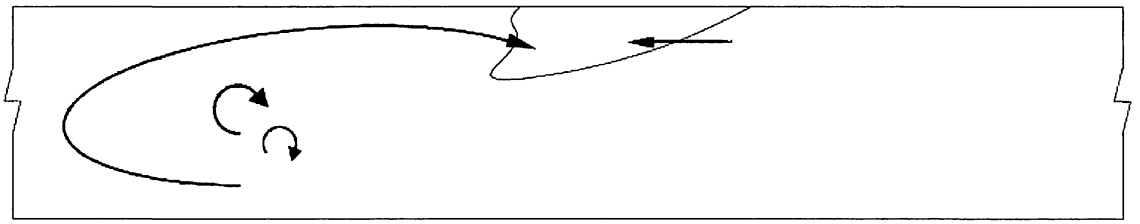

b.) Pipe filling bore formed by reflection from up-slope end of tunnel trapping an air pocket between it and the gradual flow regime transition.

Figure 1. Potential sequence of events during tunnel filling resulting in the entrapment of a large air pocket.

2 Experimental Investigation

2.1 Experimental Setup

All experiments were performed in a pipeline installed within a flume with an adjustable slope. The head box to the flume was used as a constant head reservoir and a wall was constructed across the flume entrance with the pipeline connection passing through the wall. The reservoir head H_R as reported in this report is defined as the difference in elevation between the reservoir water level and the centerline elevation of the pipe at the inlet. Although the pipeline configurations varied slightly across the different sets of experiments, the basic setup consisted of approximately 15 m of 9.4 cm-diameter clear acrylic tubing that was capped on the downstream end. A limited number of experiments at the end of the testing period utilized a shorter pipe approximately 8.8 m in length. A standard 4 inch quarter turn butterfly valve was installed at the reservoir end of the pipeline, approximately 17 cm from the upstream wall of the reservoir to the center of the valve. The pipeline was made up from approximately 2 m long tubing segments joined together by flexible rubber fittings. These allowed a slight misalignment of the segments and apparently increased the local resistance, resulting in greater energy losses within the pipeline than would be expected from the smooth pipe wall. A few steady flow tests were performed to estimate the

losses through the open valve and piping and indicated that the fully open valve loss coefficient was about 5 and the apparent friction factor for the piping was about twice that expected for a smooth pipe.

Pressures were measured with a Kistler Model 206 piezoelectric pressure transducer. Some preliminary measurements were made utilizing an Endevco 8510B-1 pressure transducer but the pressure range was inadequate for the pressures experienced in many of the experiments. One issue associated with the Kitler pressure transducer is that it does not hold a signal consistent with a step change in pressure and the pressure reading after such a change will drift back to zero over 10-20 seconds following the change. Figure 5 presented below indicates the tailing off of the pressure towards the end of the experiment, an effect that is most likely due to the transducer response. This effect will not have any consequential influence on the first maximum and minimum pressures recorded in the experiments described in the following sections. The data reported herein are all pressures measured in the air phase within the trapped air pocket. The pressure transducer was flush mounted and installed in the end cap at the downstream end of the pipeline. Measurements with the Endevco transducer were located 1.1 m from the head wall; results of those measurements are not included in this report. The signal from the transducer was directed to a National Instruments data acquisition system through a Model DAQ-Pad MIO-16XE-50 analog to digital conversion board. Measurements were generally collected at 100 Hz for a sufficient time to observe the majority of the transient. Piezometers were installed in the wall to the reservoir (to measure reservoir head) and at a bottom tap located approximately 8.75 m from the reservoir head wall.

2.2 Experimental Configurations

As explained in more detail in the results section, several different experimental setups were implemented over the course of the investigation. These involved variations in the slope and the piping configuration. Each of the configurations is documented below although detailed measurement results are not included for all of these:

- The first set of experiments involved a down-sloping pipeline with a 1 percent slope. The total pipe length was 14.25 m. The experiments were performed with an initial water level inside the pipe. The slope would produce a wedge-shaped air bubble decreasing in thickness going down the pipeline and eventually terminating within the pipe. No measurement results are presented for this configuration;
- A second set of experiments was basically the same except for the slope. In this set of experiments, the pipe was up-sloping at a grade of 0.452 percent. This produced a wedge-shaped

air pocket with maximum thickness at the downstream end of the pipe. Again, the bubble terminated within the pipe. This configuration is indicated schematically in Figure 2;

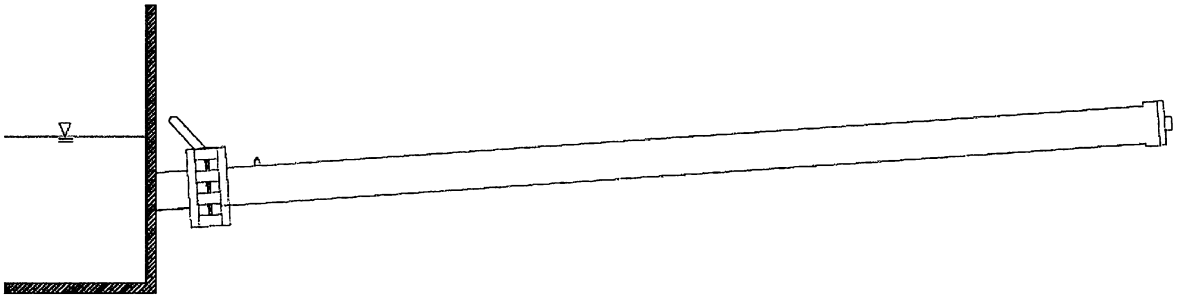

Figure 2. Experimental setup for up-sloping pipe experiments. Air is distributed along pipe crown at right end of system.

- A third configuration involved placing a short radius elbow such that the last 0.7 m of the pipeline was oriented vertically above the elbow; Figure 3 depicts this configuration schematically. Inclusion of the elbow added about 0.18 m in length measured along the inside of the bend to the pipeline length. These experiments were performed with a down-sloping pipe with a grade of 0.54 percent except that a few additional experiments were performed with a one percent slope.

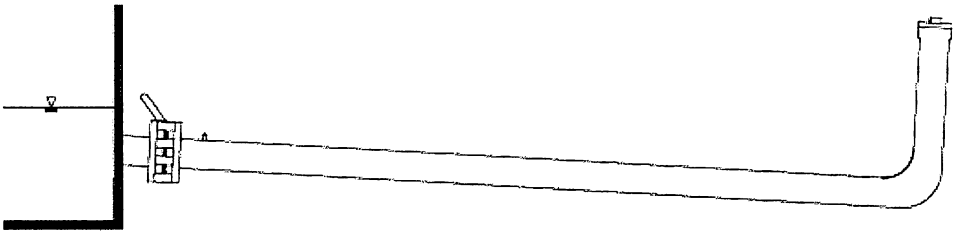

Figure 3. Experimental setup for which air is confined to the vertical riser at right end of system.

- The final configuration is depicted in Figure 4. This involved installation of a ventilation tower approximately 0.8 m from the downstream end of the pipeline. The ventilation shaft was made from 1½ inch diameter Schedule 40 PVC pipe, a size that previous experiments had indicated could vent air from the filling pipeline without a noticeable increase in air pressure. The tee fitting that the ventilation shaft was connected to increased the total pipeline length to 14.45 m. A quarter turn ball valve was connected to the shaft as close to the pipeline as possible; measurements indicated that there were 200 ml of volume between the closed valve and the crown of the pipe. These experiments were performed with an up-sloping pipe with a very small slope of 0.082 percent. At the end of the testing sequence, a shorter pipe length of 8.6 m was assembled to perform a few additional experiments to determine whether or not the length of the water column being decelerated was an important parameter.

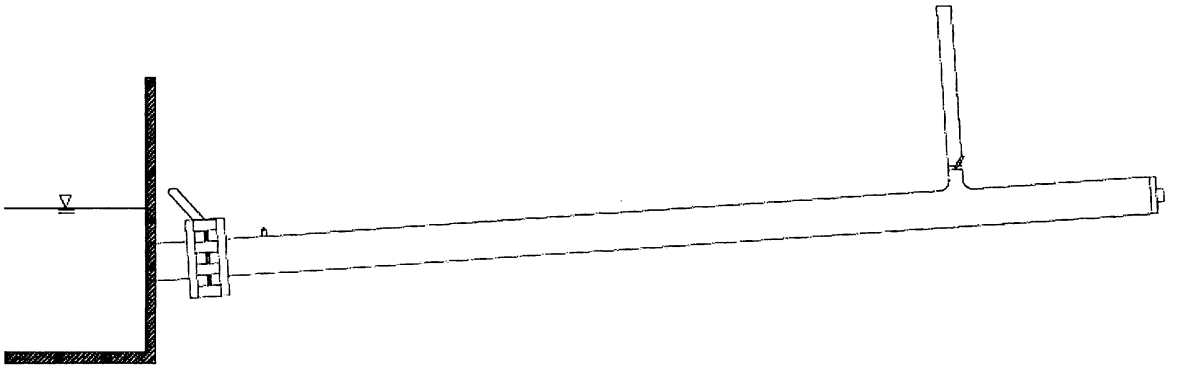

Figure 4. Experimental setup in which air ventilation is allowed through vent riser at right end of system until valve at bottom of vent riser is closed.

Each of these configurations was intended to explore a different issue in the experiments; more discussion is provide further below in the Results section to indicate the nature of the experiments performed with the various setups.

2.3 Procedure

Depending on the particular set of experiments, different variables were adjusted. These included the initial volume of air inside the pipeline or the initial water level as measured in the piezometer, and the reservoir head. All experiments were started with the upstream valve closed. There was a small air valve that could be used to ensure that the air was at atmospheric pressure prior to an experiment. Once the reservoir head and air volume/water depth was set, the data acquisition system was started. The upstream valve was then suddenly opened. The pressure data was written to a text file and could be subsequently examined to find the maximum and minimum pressures subsequent to the valve opening. Experiments were repeated at least twice to ensure consistent results. Various water depths or air pocket positions were recorded at the end of the experiment and the next test was readied to repeat the process. The air volume was estimated from the pipe geometry and the measured depth at a particular location or the length of the air wedge in the pipe. A small computation was prepared to numerically integrate the changing cross-sectional area of the air along the pipe to determine the air volume. It is noted that the position of the air bubble end is influenced by surface tension and therefore should depend on which way the bubble is moving at the end of the experiment (unknown since the flow is oscillating) and therefore the air volumes should only be considered as reasonable estimates.

The pressure record for each experiment was saved to a data file; a typical pressure trace from an experiment is indicated in Figure 5. Due to the experimental setup, the initial air pressure was atmospheric. After the upstream control valve was opened (or the valve at the riser was closed in the case of the downstream ventilation experiments), the pressure rose to a maximum value as the air pocket was compressed followed by a pressure drop and subsequent damping oscillations as the system returned to a stagnant condition. The measurements of interest in this pressure trace are the first high and low pressures that were recorded as depicted in Figure 5 which is an up-sloping pipe experiment. As mentioned the pressures were recorded at a frequency of 100 Hz. In general, signal noise may result in small deviations from a smooth pressure signal. The maximum and minimum pressures were estimated from the smooth trends in the pressure variation as opposed to individual measurements that may include some signal noise. All experimental conditions and measurement results for the three sets of experiments are provided in Appendix A. Not all of this data is presented or discussed in the Results section, but it is included in Appendix A for completeness

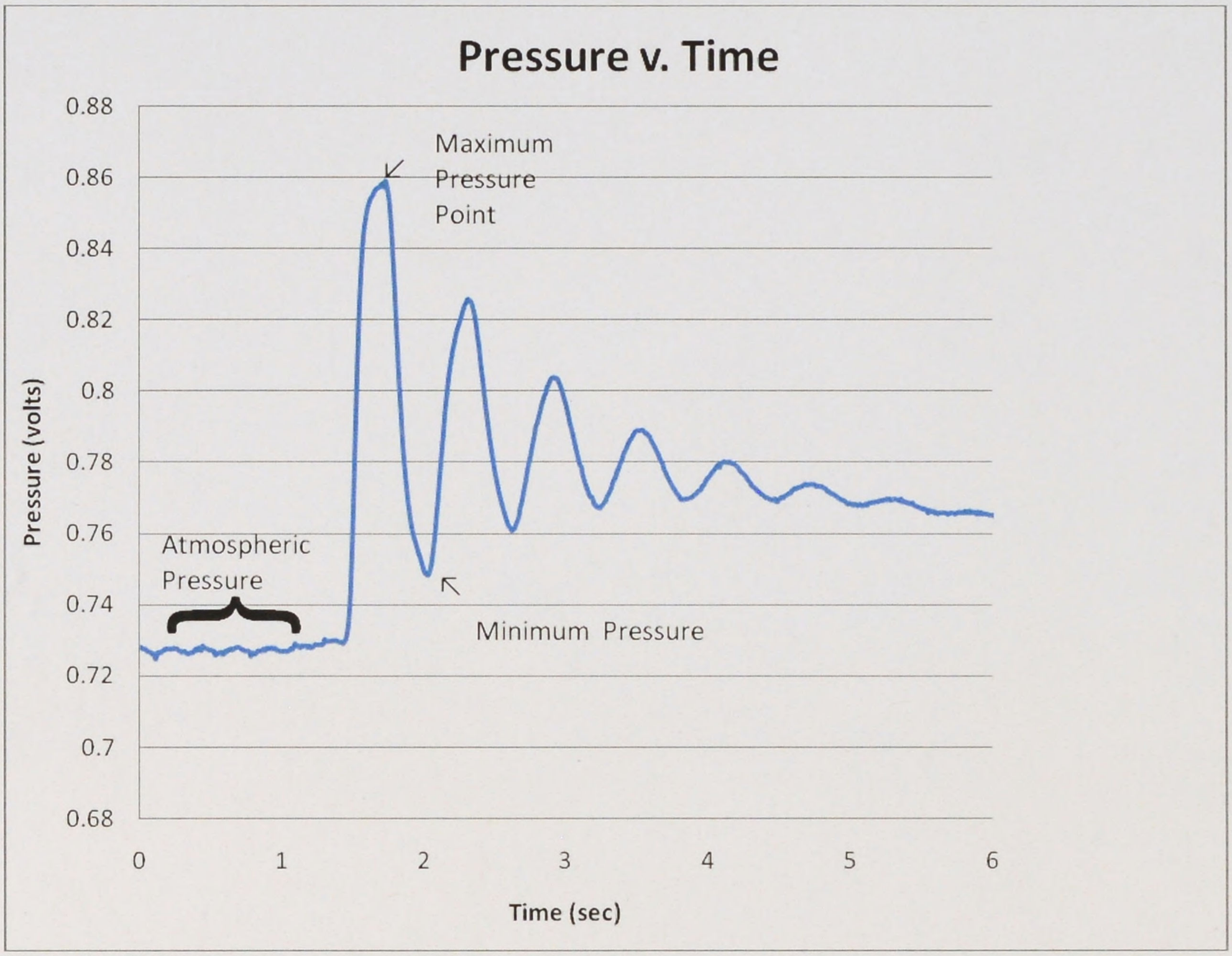

Figure 5. Typical pressure trace recorded in experiment.

3 Results

3.1 Initial experiments in down-sloping pipe

The initial set of experiments was performed with a pocket of air maintained at the upstream end of the down-sloping pipe. The original idea was that this would somewhat represent conditions that would exist following bore reflection off the upstream end of a prototype system with subsequent compression of the trapped air pocket. However, an important difference is that in the experiments, the water in the pipeline is at rest and a sudden increase in head is applied at the upstream end. Since the water was stagnant, there was nothing to prevent the air from migrating towards the reservoir along the tunnel crown as it was compressed and thus air escaped through the suddenly opened valve and into the reservoir. Under these circumstances, it was impossible to know the air volume inside the pipeline as the experiment commenced and, in fact, all air eventually vented through the pipeline entrance (although

relatively slowly compared to the pressure transient variations that occurred.) Some attempts were made to confine the air to the pipeline. These involved installing a baffle consisting of a segment (one-third of a diameter in height) of a circular area along the top of the pipe to try to prevent upstream air migration. In the first attempt, the blockage of the pipe was insufficient and air migrated past the baffle and into the reservoir as before. The height of the baffle was then increased to half the diameter and moved downstream about 1.5 meters. This baffle height prevented air from migrating upstream but these experiments were abandoned since the large degree of blockage in order to prevent upstream air migration made any interpretation of the results difficult. The pressure rises measured were fairly modest and interestingly, were similar regardless of whether or not the baffles were present.

3.2 Experiments in up-sloping pipe

The basic experimental setup was modified by adjusting the pipe slope so that the trapped air was confined at the far end of the pipeline and could not escape back through the reservoir control valve indicated in Figure 2. The pressure transducer was relocated to the downstream end of the pipeline such that it was recording pressure directly within the trapped air pocket although some preliminary measurements were made with the pressure transducer in its original position near the reservoir. The air volume was such that the trapped air resulted in a wedge that terminated somewhere within the pipe. This position was noted prior to commencing the experiment and the air volume computed from the geometry of the sloping pipeline. Results of the measurements are presented in Figures 6 and 7. Basically, both the maximum and minimum pressures increased (deviation from the initial atmospheric pressure) as the air volume was reduced and also increasing with the increased reservoir head. The minimum pressure appeared to be more influenced by air volume than the maximum pressure. These results are consistent with the analysis by Martin (1976) who used a rigid column model to predict pressure variations in a similar system. One important consideration is that the rigid column analysis basically assumes that the air is confined at the end of the pipeline and ignores the effect of slope in distributing the air along a considerable portion of the pipeline for small slopes such as investigated in this study. This effectively assumes that only the magnitude of the air volume is important and not how it is distributed along the crown of the pipeline. Since the pipeline is full at the reservoir end, no hydraulic bore formed in these experiments and it is unclear how representative the results presented will be in a prototype application with a filling scenario such as described in Section 1.3.

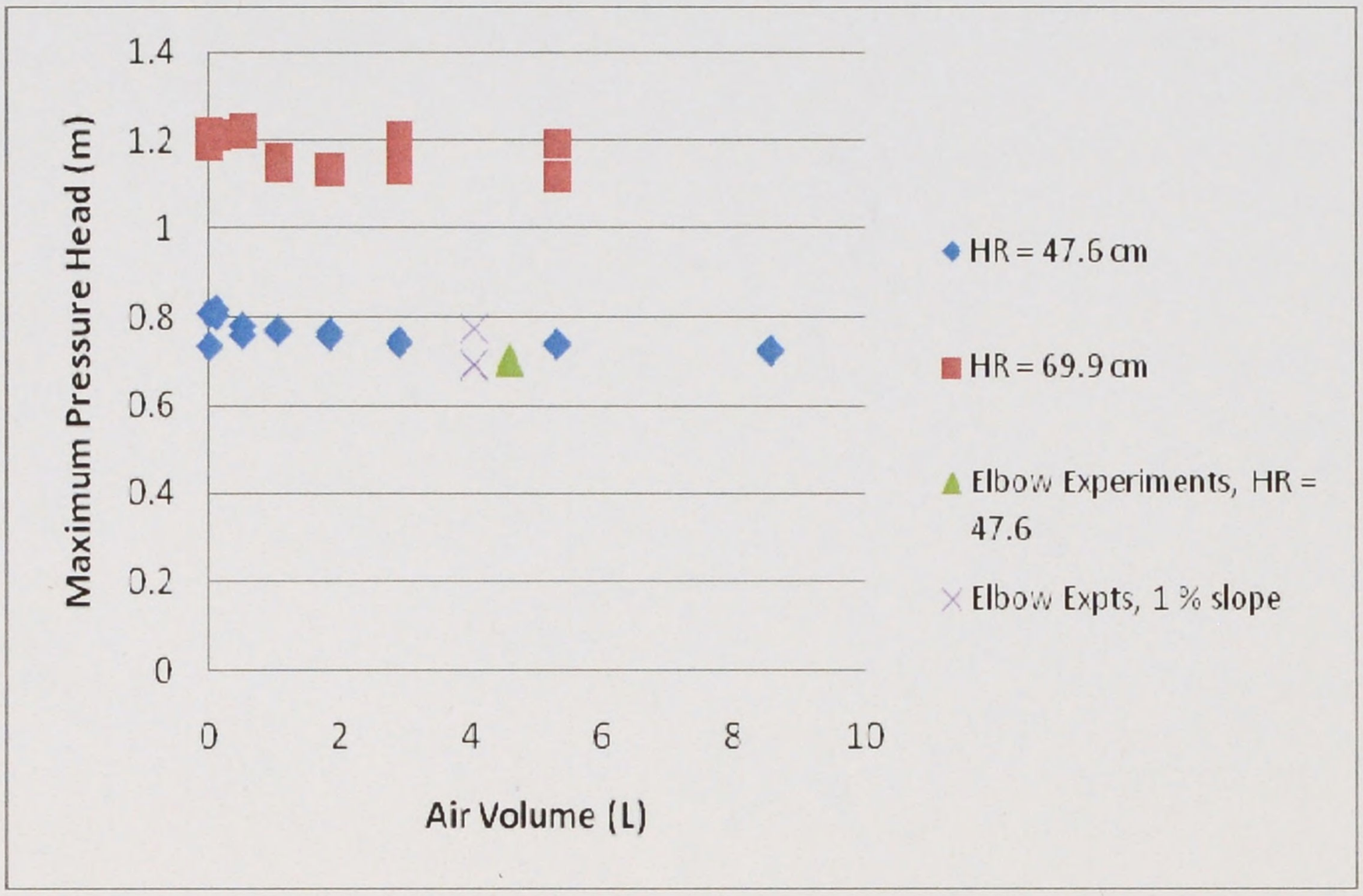

Figure 6. Maximum air pressure heads as a function of air volume.

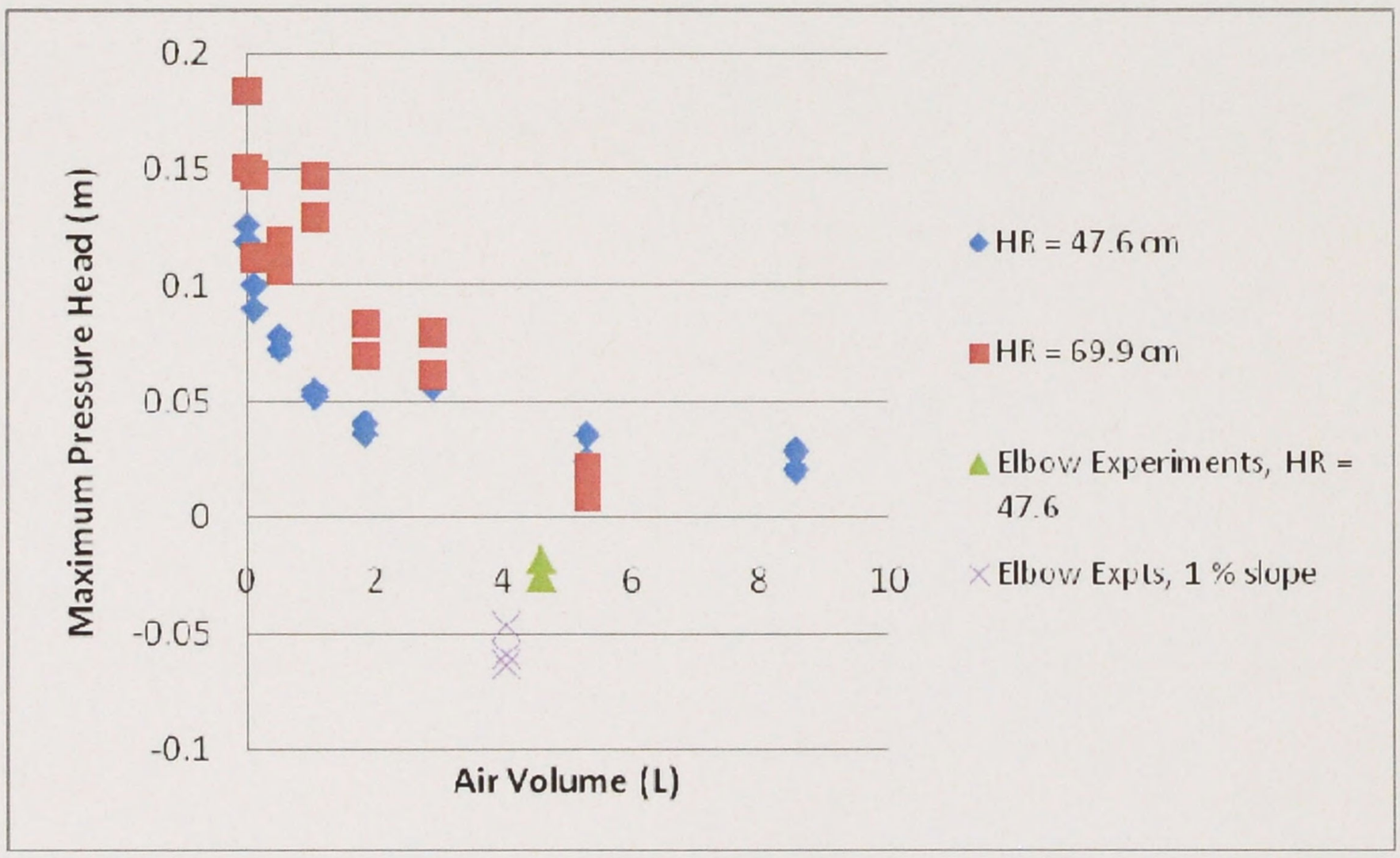

Figure 7. Minimum air pressure heads as a function of air volume.

An additional set of experiments was performed to partially address the question of whether the distribution of air along the top of the pipeline played any role in the magnitude of the pressure peaks. These experiments were performed by installing an elbow at the downstream end of the pipeline and confining the air to the vertical portion of the pipe end as depicted in Figure 2. In this configuration, the driving head (elevation between the reservoir and the air water interface in the riser decreases as the air volume decreases.) It was found that the pressure spikes decreased with decreasing air volume so that apparently the effect of decreasing air volume is more than offset by the decreasing head difference associated with that smaller air volume. Because these experiments were performed with a down-sloping pipe, there is a single air volume (for the given pipe slope) at which the head difference and the air volume matches those in the up-sloping pipe experiments. The measurements from the experimental conditions that most closely match this condition are presented on Figures 6 and 7. Roughly the same elevation difference between reservoir and downstream water levels occurred for an air volume of approximately 4.5 L. In the up-sloping pipe experiments, the maximum measured pressure head was 0.74 m while it was 0.70 m in the vertical riser with elbow experiment. The small difference may be at least partially explained by the addition of the short radius elbow which produces extra energy loss in the latter experiment. The minimum pressure does not match as well but the two systems are not quite analogous. In order to provide a little more confidence in these comparisons, a few additional experiments were performed with the pipe slope increased to one percent. These experiments were performed only for one air volume, namely the one that would yield the same total head difference as the up-sloping pipe experiments. These results are also shown in Figures 6 and 7 and support the discussion above for the smaller slope. Therefore, it is concluded that the most important issue influencing pressure rises is the total volume of air that is trapped and compressed, and not so much how it is distributed.

3.3 Numerical simulation of elbow experiments

It is relatively straightforward to perform a rigid column analysis for the elbow experiments since the air is confined to the vertical section of the downstream end of the pipe. This analysis was developed to check for unexpected results that may also apply to the other experiments. A rigid column analysis basically treats the water as incompressible. The compression of the air can be accounted for directly, basically as in the method presented in Martin (1976). A full derivation of the equations is not presented herein, and they are simply listed below in the form implemented:

$$\frac{dV}{dt} = \frac{g}{L}\left[\Delta z - \frac{P_{air}}{\rho g} - (K + \frac{fL}{D})\frac{V|V|}{2g}\right] \quad Momentum\ equation$$

$$\frac{d(\Delta z)}{dt} = -V \quad Continuity\ of\ water\ in\ riser$$

$$\frac{dV_{air}}{dt} = VA \quad Continuity\ of\ air - water\ surface$$

$$PV_{air}^{n} = Const. \quad isentropic\ compression\ relation$$

In these equations:

V = water velocity

g = gravitational acceleration

L = pipe length

Δz = the elevation difference between the reservoir surface and the water level in the downstream riser

P_{air} = air pressure, defined as relative to atmospheric in the momentum equation but must be as a absolute pressure in the isentropic relation

ρ = water density

K = sum of all local loss coefficients for the pipeline

f = Darcy-Weisbach friction factor

V_{air} = air volume

A = pipe cross-sectional area

n = specific heat ratio (equal to 1.4 for air)

These equations were solved utilizing a simple Euler numerical integration scheme starting from an initial head difference and the water at rest, but assuming that the full reservoir head was instantaneously applied to the column of water in the pipe. Figure 8 shows a comparison between the predictions for the experiment presented in Figures 6 and 7 for the 0.54 % slope. In this comparison, notice that the pressures at the end of the measurement tend to oscillate about zero pressure as opposed to the reservoir head; this is due to the performance characteristic of the pressure transducer as discussed above. The first

maximum and minimum pressures are simulated fairly well although the predictions suggest a slightly higher pressure than the observed value. This outcome was consistent for all the other experiments that were analyzed. The more important factor in this figure is that the experimental pressure oscillations decayed much more rapidly than the predicted ones. In the simulation the *K* value assigned was 7 and the Darcy-Weisbach friction factor used was 0.5, consistent with the estimates from the steady state measurements. The *K* value needed to be increased to about 300 in order for the oscillation decay to match the observations, a quite unrealistic result. We have observed in experiments in the past that predicted inertial oscillations do not decay as rapidly as measurements, but the effect seems quite pronounced in this situation. In the past, attempts have been made to include frequency dependent friction in the analysis, but the effect at the time scale of inertial oscillations has been small. These results point to the possibility of additional, unaccounted for energy losses in these experiments. Nevertheless, when the loss coefficient was assigned a value of 300 that would provide a good reproduction of the amplitude decay, the prediction of the maximum pressure matches quite closely with the measurement. This outcome was similar for the other experiments simulated as well. The period of oscillation is also well predicted. A conclusion is that numerical models to predict any of the results of this study may need to include larger losses than might have been anticipated. The reason for this is not clear.

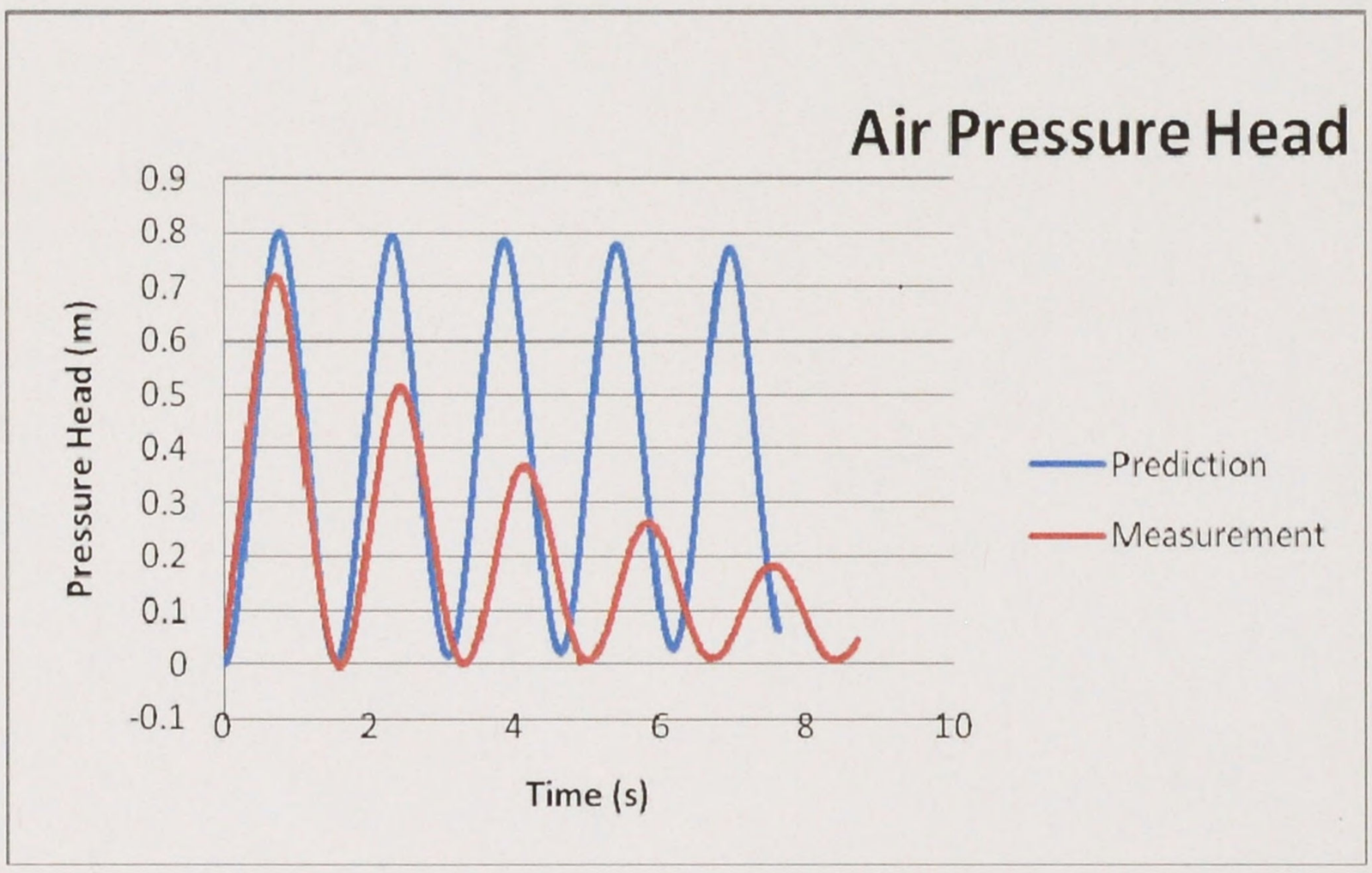

Figure 8. Comparison of predicted and measured pressure heads in elbow experiments using rigid column model.

3.4 Bore interaction experiments

Since the filling scenario described in Section 1.3 involves the interaction when an advancing hydraulic bore compresses the air in a trapped pocket, it is unclear that the results presented above are suitable to understand the magnitude of maximum and minimum transient pressures to be expected in a prototype system. In particular, the water is initially at rest and then begins to compress the air while it is beginning to accelerate, thereby stopping the flow before it really has a chance to achieve any speed. On the other hand, the filling scenario that is described will result from the reflection of an upstream propagating bore and therefore the equilibrium bore velocity could easily be on the order of 10 m/s or more in a prototype system. It was with this issue in mind that the last set of experiments was designed. Specifically, we wanted to provide a mechanism for a strong bore to develop and the only way visualized to accelerate the fluid from rest was to initially allow the air to escape. The ventilation riser valve was closed only once the bore was well established. Although the exact amount of air in the system could not be pre-determined for any individual experiment, it was possible to measure the air volume remaining in the system following the experiment. By performing the experiment in an up-sloping pipe (but with a very small slope of 0.00082), the air would tend to remain towards the downstream end of the pipeline although it would gradually propagate upstream against the pipe slope. By recording the position of the end of the air bubble at the completion of the experiment or the water depth at a reference location, it was possible to estimate the air volume remaining in the system (although probably not with a high degree of precision.) The majority of the experiments were performed with two different reservoir heads and two different initial water depths so that the effect of two variables that would influence the strength of the bore could be established. A few additional experiments were performed at other sets of conditions but these were not analyzed in detail in this report with one exception as noted in the discussion below. In particular, the higher the reservoir head and the higher the initial water level in the pipeline, the stronger the hydraulic bore should be. Results as presented in Figs. 9-12 confirm that higher pressure rises result from stronger bore conditions and also re-confirm that the pressure rises are greater for smaller trapped air volumes. Figures 9 and 10 present the results for a single initial water depth at two different reservoir heads while Figures 11 and 12 present results for a single reservoir head at two different initial water depths. It is seen that the pressure rises are substantially greater than for the previous experiments discussed above which is not unexpected since the nature of the experiment provides an opportunity for the flow to accelerate more before the air compression begins and the higher flow inertia requires a greater air compression to stop it. The effect of initial reservoir head is seen as being less important than the effect of initial depth. Visually, the bore speeds were greater with the larger initial depth suggesting that the bore speed is an important influence in determination of the pressure rise.

These experiments also indicate substantial sub-atmospheric pressures which was not noted in the previous sets of experiments where the minimum pressures either remained above atmospheric (sup-sloping pipe experiments) or slightly sub-atmospheric (elbow-riser experiments). In some sense, this is to be expected since the pressure oscillations indicated in Figure 5 start out at atmospheric pressure. Even though the minimum pressure oscillation does not deviate as much from the mean trend line of the pressure variation, the stronger swings in pressure will tend to carry it below atmospheric pressure.

If the remaining data is examined in pairs similar to those presented in Figures 9-12, similar trends emerge.

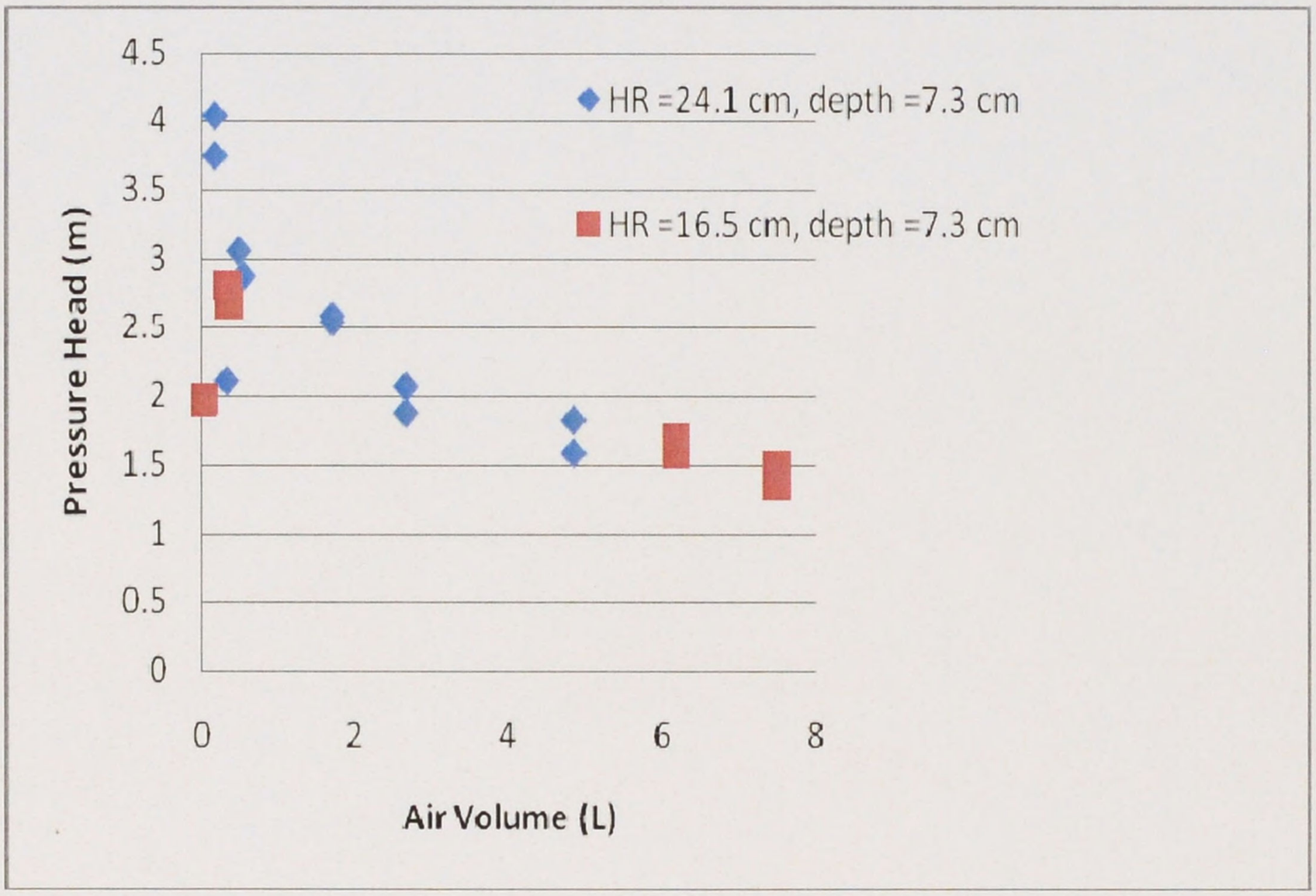

Figure 9. Maximum pressures versus air volume for constant depth, variable reservoir head.

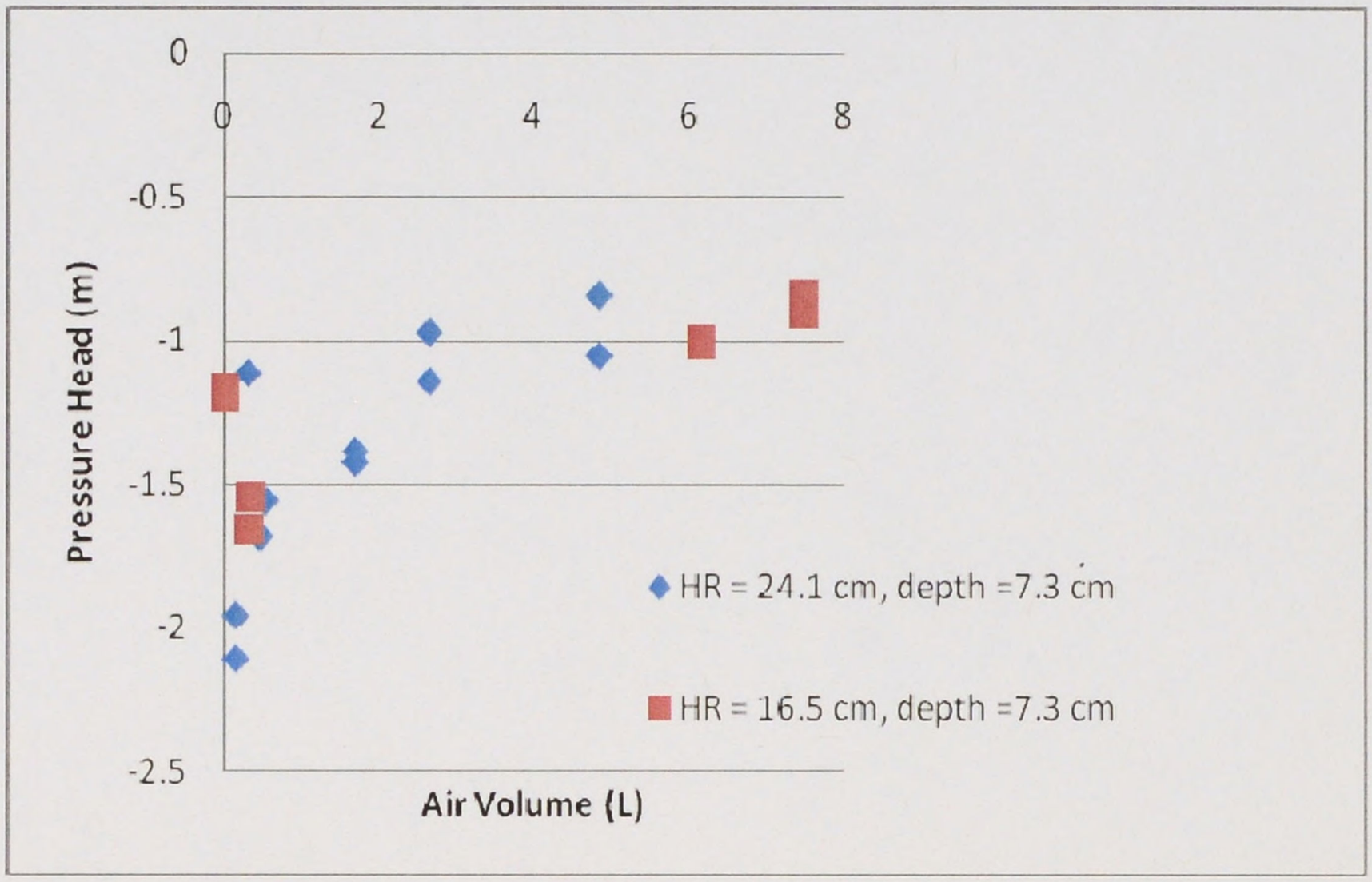

Figure 10. Minimum pressures versus air volume for constant depth, variable reservoir head.

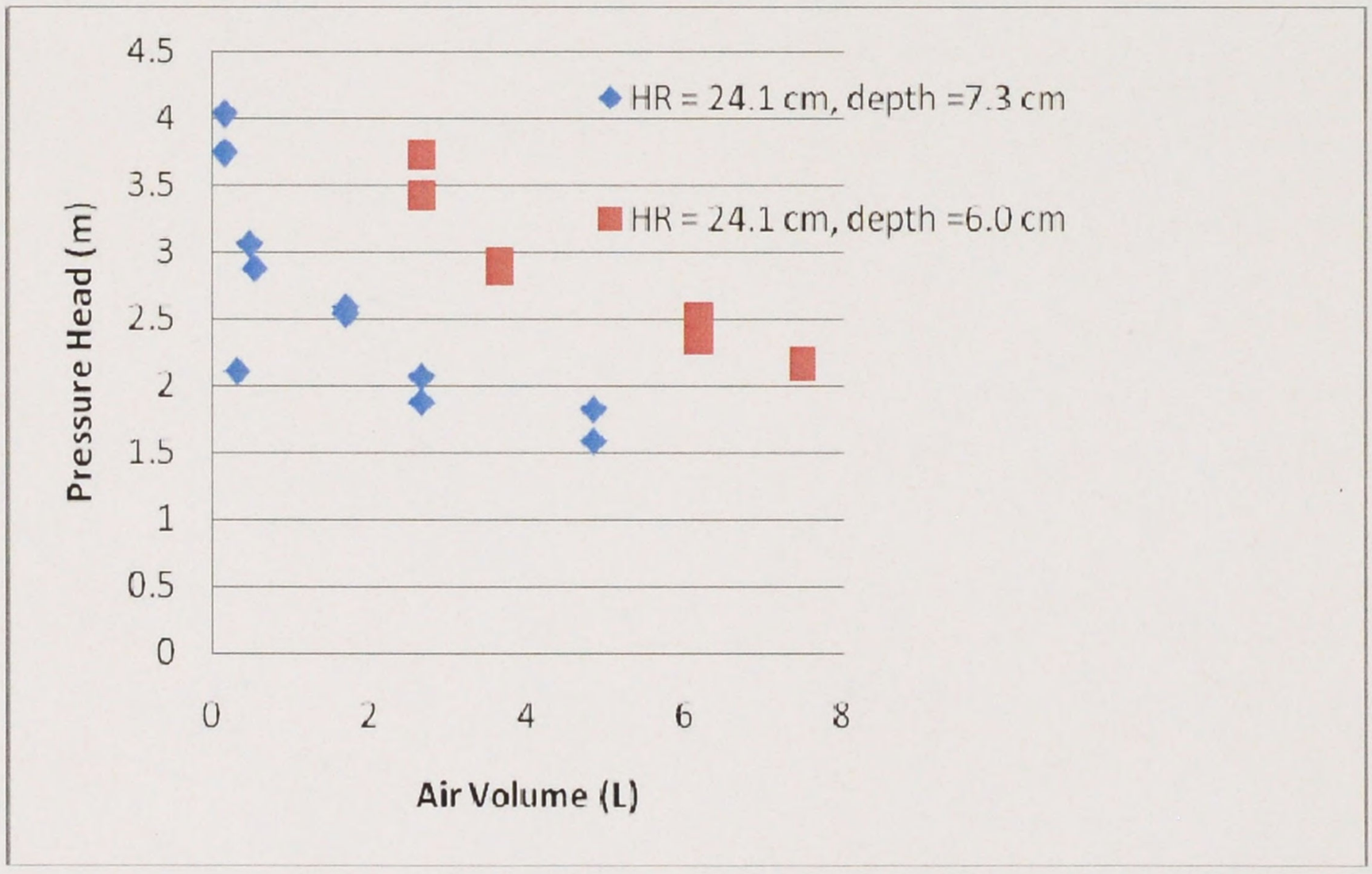

Figure 11. Maximum pressures versus air volume for constant reservoir head, variable depth

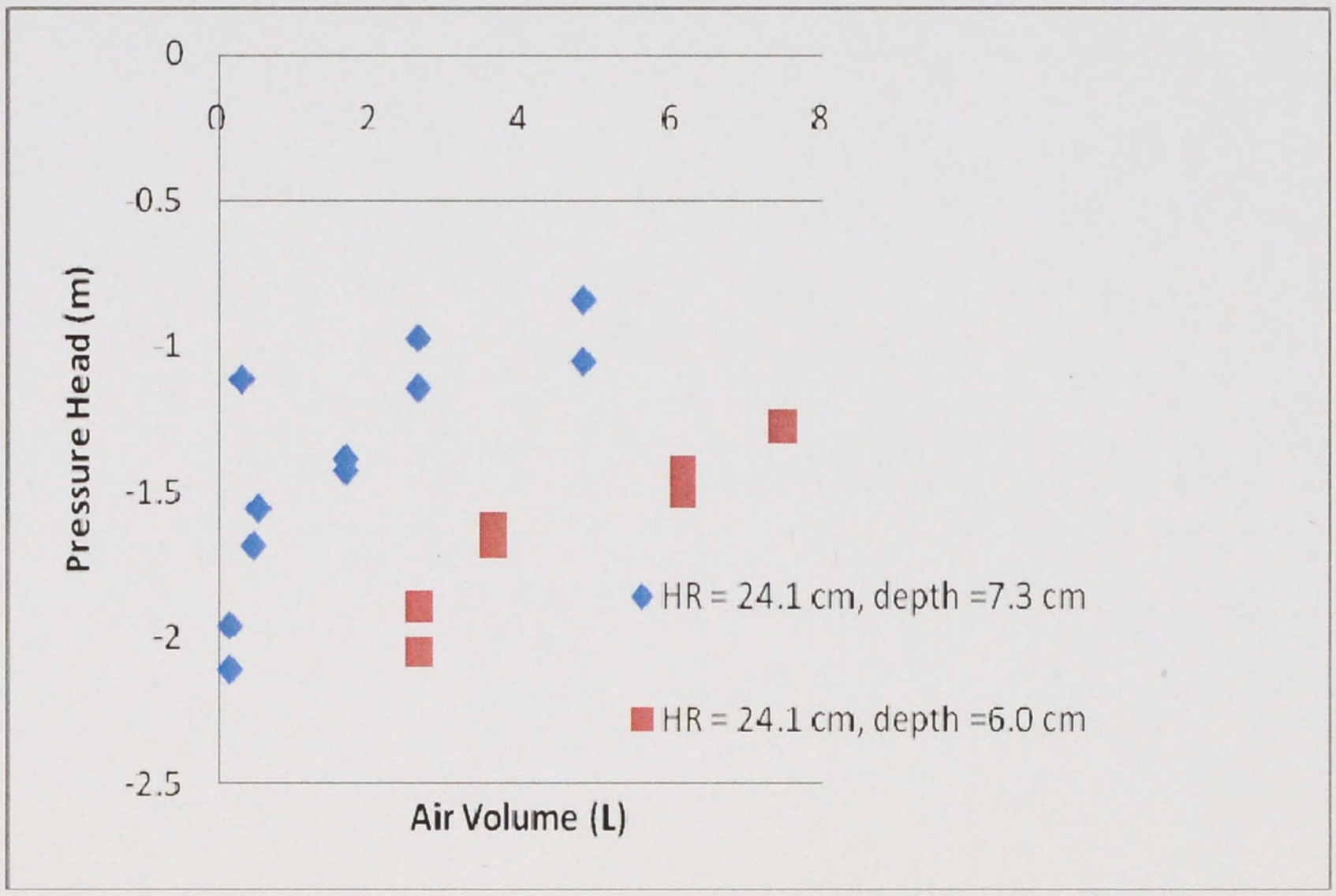

Figure 12. Minimum pressures versus air volume for constant reservoir head, variable depth.

Since the experiments are at best an idealization of a prototype system, some methodology is desirable to extrapolate these results to actual applications. One approach to this is to present the results in a dimensionless format. Unfortunately, there are too many variables to perform a dimensional analysis and develop simple relationships. Therefore an approximate analysis based on a heuristic analysis of the flow was developed to guide the development of a dimensionless presentation. Even this requires some simplifying assumptions such that the final results will only attempt to capture the general effects of the important variables. We start with a simple system as indicated in Figure 13 with a pipe-filling bore propagating at a constant speed c from a reservoir of constant head H_R in a horizontal pipeline with stagnant initial conditions and a constant initial depth. In order for the bore to propagate at a constant speed, one must neglect all energy losses. Continuity and momentum equations in the frame of reference of the bore for a control volume that surrounds the bore are as follows:

$$(c - V_1)A = cA_0$$

$$\rho(c - V_1)^2 A + P_1 A = \rho c^2 A_0 + P_0 A_0$$

In which V_1 and P_1 are the velocity and pressure behind the bore, respectively, A is the full cross-sectional area of the pipe, and A_0 and P_0 are the area and pressure ahead of the bore. In order to proceed, it is assumed that P_1 is approximated by ρgD (with D the pipe diameter) which implies that the bore is only slightly surcharged and that the reservoir pressure head is converted mainly into kinetic energy and that P_0 is sufficiently small to be neglected relative to the other terms. Algebraic manipulation of the two equations with these assumptions yields an expression for c as:

$$c^2 = gD\frac{A^2}{A_0(A-A_0)}$$

The air compression process is assumed to represent a conversion of the bore energy into air pressure as:

$$\rho c^2 \propto P_{\max}$$

The non-dimensional parameter to present either the maximum or minimum pressure P_{max} or P_{min} is thus:

$$\frac{P_{\max} or P_{\min}}{\rho gD\ \dfrac{A^2}{(A_0(A-A_0)}} = f(\frac{V_{air}}{D^3})$$

In which V_{air} is the initial air volume and D is the pipe diameter. The second dimensionless parameter comes directly from the intuitive notion that the length of pipe occupied by the trapped air pocket is the key dimensionless variable describing air pocket volume. Although this expression involves several approximations, the presentation in Figures 14 and 15 suggests that it does a reasonably good job of collapsing the experimental data. The data scatter at small initial air volumes is likely to be controlled by the very approximate way in which the air volumes were estimated in these experiments as discussed previously. Further investigation would be required to verify the formulation over a wider range of variables (mainly initial water depth) but it seems appropriate as an initial representation of the experimental results. Note that the formulation is relatively straightforward to apply to a prototype application as the TPA model of Vasconcelos, et al (2006) is capable of predicting both the conditions ahead of the bore (A_0) and the air volume that is trapped in front of it. With these parameters, Figures 14 and 15 can be entered to estimate the maximum and minimum pressures associated with the transient event.

There are a few implications of the dimensional analysis that bear commenting on. First of all, the pipe diameter D is used as the relevant length scale in non-dimensionalizing the pressure rather than the reservoir head, H_R for example. The assumption employed suggests that it really should be the surcharge pressure head behind the bore that is used in the analysis, a quantity that was not measured but the experiments were designed to have relatively low surcharge pressure heads. Experiments performed over a wider range of pressure heads suggest that the reservoir head does have a minor effect of the results. A more important issue is that the total inertia of the water column is not included anywhere in the dimensional analysis. If it is true that the length of the water column behind the bore is not important, this opens up the possibility of predicting pressures from the dimensionless relations using only local parameters such as might be available from a numerical simulation that did not explicitly describe the air compression (such as the Vasconcelos, et al, 2006 model) In order to test this possibility, an additional set of experiments were performed with a shorter pipe with a total length of 8.8 m as opposed to the original 14.45 m or about a 40 percent reduction in length. All other experimental conditions were otherwise the same. The results of these additional experiments are also presented in Figures 14 and 15 and are consistent with the measurements in the original length pipe although perhaps indicating slightly larger pressures rather than smaller ones if the total water mass were important. This outcome tends to lend support to the heuristic argument used to generate the dimensionless pressure relations.

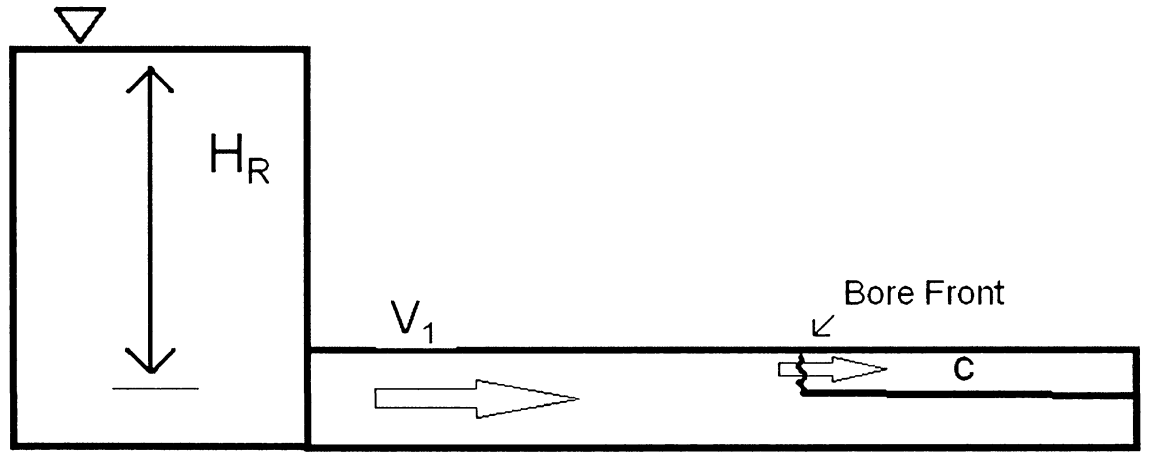

Figure 13. Definition sketch for bore propagation.

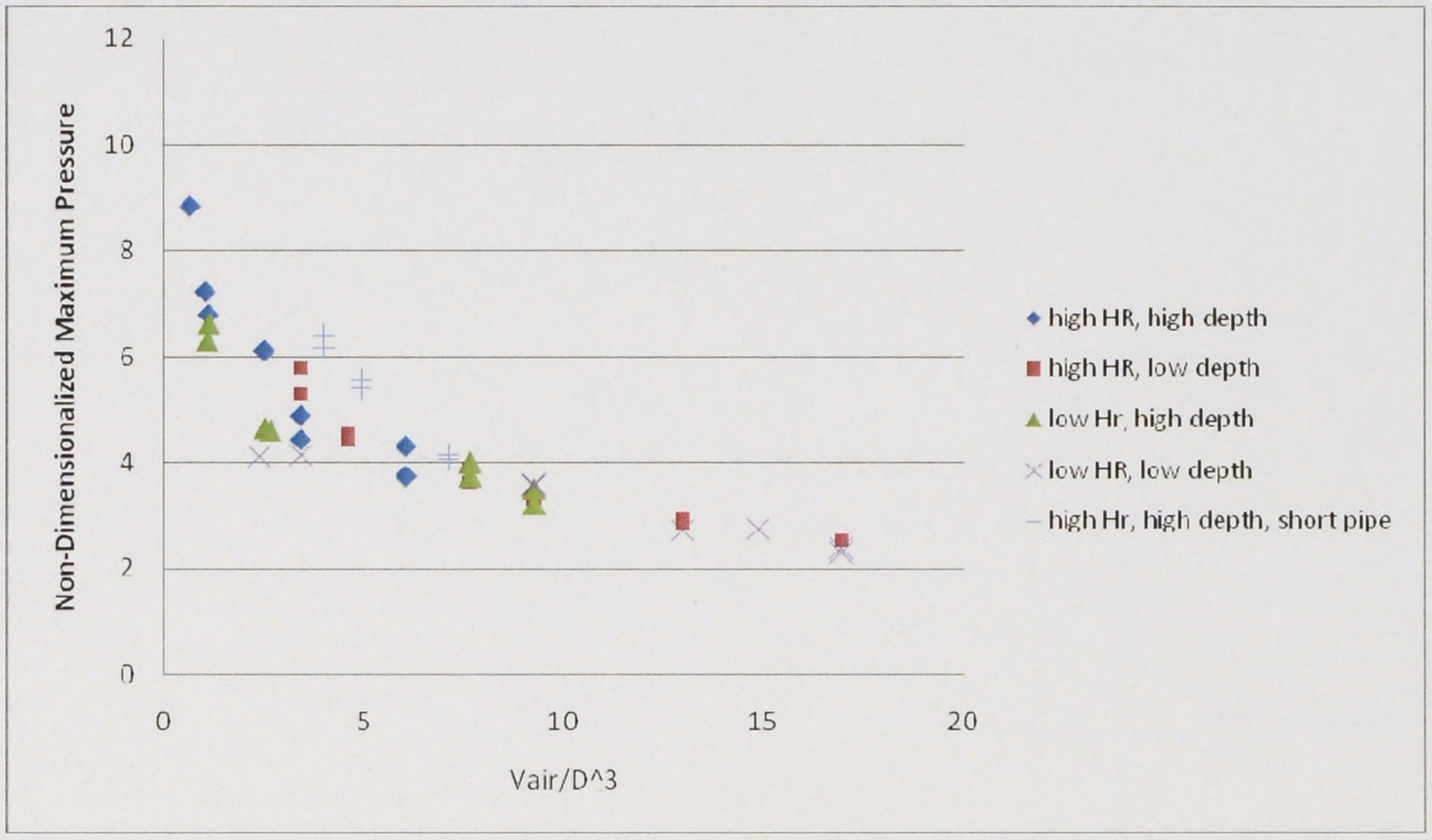

Figure 14. Presentation of dimensonless maximum pressures versus dimensionless air volume.

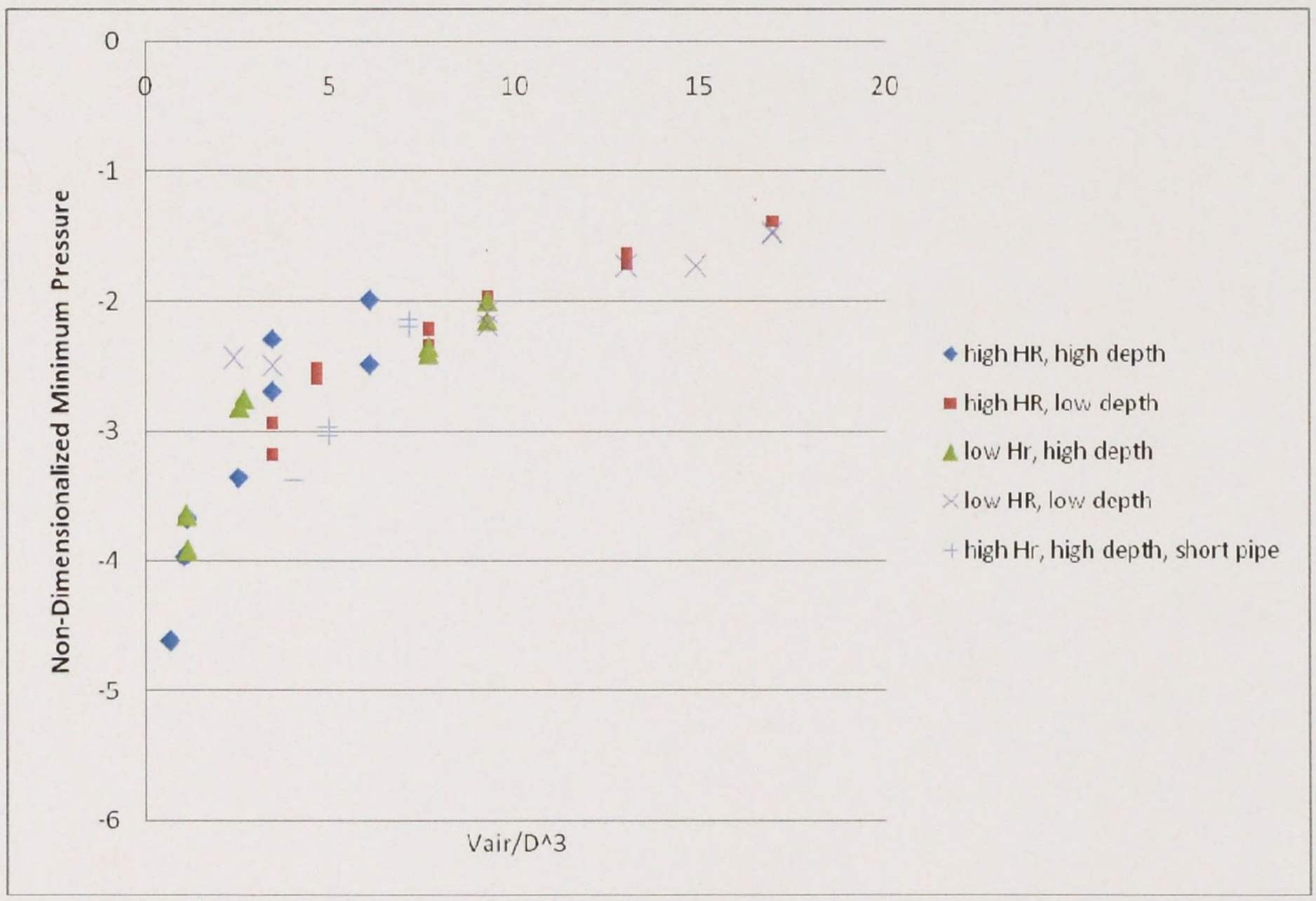

Figure 15. Presentation of dimensonless minimum pressures versus dimensionless air volume.

4 Conclusions

Preliminary experiments were performed in which the water in the system was initially stagnant and the trapped air began to compress as soon as the control valve was opened. A hydraulic bore could not form under these circumstances, resulting in relatively weak transients. This experimental setup was determined to not be representative of the filling scenario for prototype systems that is described in Section 1.3. Conclusions from these experiments include:

- As the trapped air volume became smaller, everything else being the same, the pressure rises increased, but these increases are modest;
- There did not appear to be any significant difference whether the air was distributed along the crown of the pipe as opposed to being confined to the downstream end of the pipe with similar pressure peaks and inertial oscillation periods in both sets of experiments;
- Minimum system pressures were above atmospheric or only slightly below.
- A rigid column analysis specifically developed to simulate the experiments in which the air was trapped in the vertical portion of the pipe beyond the downstream elbow was reasonably successful at predicting the peak pressures observed in those experiments as well as the inertial oscillation periods. One finding that was a bit unexpected but somewhat consistent with observations in related experiments is that the experiments showed a much more pronounced damping of the pressure oscillations than the numerical predictions. Unrealistically high energy loss coefficients would be required to match the decay in the pressure amplitudes, suggesting that some other mechanism may be producing energy losses in these experiments. If the loss coefficient was arbitrarily adjusted to produce a consistent pattern of oscillation decay, then the peak pressures were quite well predicted.

In order to perform more representative experiments, the experimental configuration was revised. A ventilation shaft with a valve located at its base was installed near the downstream end of the pipeline. Experiments were initiated with this valve in the open position so that air could escape from the pipeline; this resulted in the formation of a pipe-filling bore that pushed the air ahead of it and through the ventilation shaft. The valve was rapidly closed to trap an unknown (but measureable) volume of air within the pipe ahead of the advancing bore. Since the water flow had more opportunity to accelerate in this configuration, substantially greater pressures were observed during the compression of the trapped air that remained in the pipeline following valve closure. Findings from this set of experiments were:

- Much higher pressure rises were observed in this set of experiments, even though the reservoir heads were smaller than the previous experiments; this is attributed to the fact that the experimental setup allowed the hydraulic bore to become well established prior to the air compression, a situation that is consistent with the air entrapment scenario described in Section 1.3.
- Again, the smaller the trapped air volume, the greater the initial pressure rise with a more pronounced effect in these experiments;
- In addition, minimum pressures following the rebound of the compressed air behaved in a similar fashion in that more sub-atmospheric pressures (lower minimum absolute pressure) were observed when the initial peak pressure was higher;
- Minimum pressures observed were substantially below atmospheric, which is reasonable to expect since the initial air pressure in the system is atmospheric, the maximum pressure rise on air compression goes above atmospheric and the subsequent pressure drop with the rebound of the compressed air dropping the pressure below the equilibrium state;
- The magnitude of the pressure variations also depended on the strength of the bore which could be controlled by varying both the initial water depth in the pipe or the reservoir head with greater pressure variations associated with stronger bores. The effect of initial depth was much more significant than that of the initial reservoir head;
- A method for non-dimensionalizing the experimental data was useful in describing the observed variation in the pressure peaks, both maxima and minima. . A review of the experimental results suggests that the water mass behind the bore is not a key parameter in controlling pressure rises, a fact that would make it easier to apply to numerical predictions where only local variable would be necessary to estimate the pressure rise.
- This non-dimensionalization provides a potential framework for scaling the laboratory results to prototype applications, but only for dynamic situations that are analogous to those performed in the experiments.

Since the pressure variations observed in this study are quite large, a critical question relates to their applicability to prototype applications. If the pressure fluctuations in the first sets of experiments are compared to those in the last set, they are about an order of magnitude smaller and would probably not be judged to be problematic in many applications. What is indicated, however, is that the nature of the air compression process is extremely important. If a bore in a nearly full pipe that is propagating into a pipe at atmospheric pressure suddenly has the access to ventilation closed off, it is expected that this strong

inertia can result in extreme pressures. That was the presumption in the design of the latter experiments conducted and it would be important to verify that conditions could exist within a filling tunnel that would allow this occurrence.

5 References

Capart, H., Sillen, X., and Zech, Y. (1997). Numerical and Experimental Water Transients in Sewer Pipes. J. Hydr. Res. 35 (5), 659-670.

Cardle, J.A. and Song, C.S.S. (1988). Mathematical Modeling of Unsteady Flow in Storm Sewers. Int. J. Eng. Fluid Mechanics, 1(4), 495-518.

Martin, C.S. (1976) "Entrapped Air in Pipelines" 2nd International Conference of Pressure Surges, BHRA, F2-15 – F2-25.

Politano, M., Odgaard, A.J., and Klecan, W. (2007). Case Study: Numerical Evaluation of Hydraulic Transients in a Combined Sewer Overflow Tunnel System J. Hydr. Engrg., 133 (10) 1103-1110.

Vasconcelos, J.G., Wright, S.J. and Roe, P.L. (2006). Improved Simulation of Flow RegimeTransition in Sewers: Two-Component Pressure Approach. J. Hydr. Engrg., 132,(6),_2006, 553-562.

Vasconcelos, J.G. and Wright, S J. (2009). Investigation of Rapid Filling of Poorly Vented Stormwater Storage Tunnels" J. Hydr. Res. Vol. 47 (5), 547-558.

Wright, S.J. , Creech, C.T., Lewis, J.M. and Vasconcelos, J. G. (2008) "Mechanisms of Flow Regime Transition in Rapidly Filling Stormwater Storage Tunnels," Journal of Environmental Fluid Mechanics, 8, 605-616.

Zhou, F., Hicks, F. E., and Steffler, P. M. (2002). Transient flow in a rapidly filling horizontal pipe containing trapped air. J. Hydr. Engrg., 128(6), 625-634.

Appendix A. Experimental Conditions and Results

Up-sloping Experiments

Upslope 46A	-0.4520%	47.6	0.010563	0.809722	0.12547
Upslope 46B	-0.4520%	47.6	0.010563	0.735855	0.118564
Upslope 43A	-0.4520%	47.6	0.11391	0.817813	0.089669
Upslope 43B	-0.4520%	47.6	0.11391	0.804382	0.099872
Upslope 39A	-0.4520%	47.6	0.511677	0.78148	0.072469
Upslope 39B	-0.4520%	47.6	0.511677	0.760313	0.077749
Upslope 36A	-0.4520%	47.6	1.056787	0.768138	0.054625
Upslope 36B	-0.4520%	47.6	1.056787	0.773671	0.05228
Upslope 33A	-0.4520%	47.6	1.846167	0.75739	0.0405
Upslope 33B	-0.4520%	47.6	1.846167	0.767709	0.036189
Upslope 30A	-0.4520%	47.6	2.902758	0.746102	0.05791
Upslope 30B	-0.4520%	47.6	2.902758	0.741408	0.05603
Upslope 25A	-0.4520%	47.6	5.306241	0.742351	0.03559
Upslope 25B	-0.4520%	47.6	5.306241	0.737029	0.024641
Upslope 20A	-0.4520%	47.6	8.566733	0.727446	0.020686
Upslope 20B	-0.4520%	47.6	8.566733	0.722634	0.028815
Upslope 46A	-0.4520%	69.9	0.010563	1.190796	0.183552
Upslope 46B	-0.4520%	69.9	0.010563	1.216276	0.150505
Upslope 43A	-0.4520%	69.9	0.11391	1.210356	0.147399
Upslope 43B	-0.4520%	69.9	0.11391	1.215882	0.111848

Upslope 39A	-0.4520%	69.9	0.511677	1.215707	0.106048
Upslope 39B	-0.4520%	69.9	0.511677	1.228847	0.118622
Upslope 36A	-0.4520%	69.9	1.056787	1.159234	0.128917
Upslope 36B	-0.4520%	69.9	1.056787	1.141908	0.14704
Upslope 33A	-0.4520%	69.9	1.846167	1.130936	0.083176
Upslope 33B	-0.4520%	69.9	1.846167	1.13869	0.069546
Upslope 30A	-0.4520%	69.9	2.902758	1.137412	0.060954
Upslope 30B	-0.4520%	69.9	2.902758	1.209113	0.079359
Upslope 25A	-0.4520%	69.9	5.306241	1.120317	0.021349
Upslope 25B	-0.4520%	69.9	5.306241	1.193672	0.009174

Elbow/Vertical Riser Experiments

Elbow 19A	0.5376%	47.6	209.7422	0.703411	-0.01854
Elbow 19B	0.5376%	47.6	209.7422	0.698614	-0.02615
Elbow 16A	0.5376%	47.6	176.625	0.542306	-0.01252
Elbow 16B	0.5376%	47.6	176.625	0.559814	-0.01471
Elbow 13A	0.5376%	47.6	143.5078	0.308417	-0.00726
Elbow 13B	0.5376%	47.6	143.5078	0.447283	0.001056
Elbow 10A	0.5376%	47.6	110.3906	0.298141	0.004408
Elbow 10B	0.5376%	47.6	110.3906	0.31383	-0.00016
Elbow 7A	0.5376%	47.6	77.27344	0.149435	0.004257
Elbow 7B	0.5376%	47.6	77.27344	0.184327	0.000322
Elbow 1% 16A	1.0000%	47.6	176.625	0.773079	-0.04172
Elbow 1% 16B	1.0000%	47.6	176.625	0.690539	-0.04492
Elbow 1% 16C	1.0000%	47.6	176.625	0.692885	-0.03301

Vented Experiments

Name	% Slope	Reservoir Head (cm.)	Final Air Volume (liters)	$P_{max\,(m)}$ (pressure head)	$P_{min\,(m)}$ (pressure head)
Close Valve 6 - 42A	0.0818%	24.1	0.56582	3.747751	-1.95642
Close Valve 6 - 42B	0.0818%	24.1		4.038255	-2.10706
Close Valve 6 - 39A	0.0818%	24.1	0.878795	3.060139	-1.68126
Close Valve 6 - 39B	0.0818%	24.1	0.942366	2.876477	-1.55651
Close Valve 6 - 36A	0.0818%	24.1	2.098644	2.586193	-1.42421
Close Valve 6 - 36B	0.0818%	24.1		2.53605	-1.38544
Close Valve 6 - 33A	0.0818%	24.1	2.857219	2.064923	-1.14196
Close Valve 6 - 33B	0.0818%	24.1		2.10496	-1.11371
Close Valve 6 - 30A	0.0818%	24.1	2.857219	1.87344	-0.97106
Close Valve 6 - 30B	0.0818%	24.1	5.040283	1.820354	-1.05339
Close Valve 6 - 25A	0.0818%	24.1	5.040283	1.58203	-0.84265
Close Valve 6 - 25B	0.0818%	24.1		1.604381	-0.85914
Close Valve 5.5 - 42A	0.0818%	24.1	2.857219	3.4137	-1.89261
Close Valve 5.5 - 42B	0.0818%	24.1	2.857219	3.731922	-2.0482
Close Valve 5.5 - 39A	0.0818%	24.1	3.839908	2.919463	-1.67507
Close Valve 5.5 - 39B	0.0818%	24.1	3.839908	2.85205	-1.62319
Close Valve 5.5 - 36A	0.0818%	24.1	6.361436	2.517312	-1.50603
Close Valve 5.5 - 36B	0.0818%	24.1	6.361436	2.339266	-1.42804
Close Valve 5.5 - 33A	0.0818%	24.1	7.681857	2.142194	-1.26952

Close Valve 5.5 - 33B	0.0818%	24.1	7.681857	2.172147	-1.28342
Close Valve 5.5 - 30A	0.0818%	24.1	10.78767	1.836633	-1.05401
Close Valve 5.5 - 30B	0.0818%	24.1	10.78767	1.890501	-1.10257
Close Valve 5.5 - 25A	0.0818%	24.1	14.06864	1.631408	-0.89234
Close Valve 5.5 - 25B	0.0818%	24.1		1.637085	-0.89397
Close Valve 6 - 42A	0.0818%	16.5	0.910157	2.67148	-1.54376
Close Valve 6 - 42B	0.0818%	16.5	**0.942366**	2.810389	-1.65864
Close Valve 6 - 39A	0.0818%	16.5	**2.098644**	1.970414	-1.19313
Close Valve 6 - 39B	0.0818%	16.5	2.214685	1.953811	-1.1664
Close Valve 6 - 33A	0.0818%	16.5	6.361436	1.588397	-0.99668
Close Valve 6 - 33B	0.0818%	16.5	6.361436	1.696495	-1.01744
Close Valve 6 - 30A	0.0818%	16.5	7.681857	1.361337	-0.84335
Close Valve 6 - 30B	0.0818%	16.5	7.681857	1.487793	-0.90934
Close Valve 5.5 - 42A	0.0818%	16.5	1.98666	2.653993	-1.57082
Close Valve 5.5 - 42B	0.0818%	16.5	2.857219	2.67105	-1.60722
Close Valve 5.5 - 39A	0.0818%	16.5	7.681857	2.301167	-1.3463
Close Valve 5.5 - 39B	0.0818%	16.5	7.681857	2.316817	-1.40662
Close Valve 5.5 - 33A	0.0818%	16.5	12.33562	1.76897	-1.11378
Close Valve 5.5 - 33B	0.0818%	16.5	10.78767	1.747213	-1.11472
Close Valve 5.5 - 30A	0.0818%	16.5	14.06864	1.534525	-0.94589
Close Valve 5.5 - 30B	0.0818%	16.5	14.06864	1.478204	-0.95438
Close Valve 6 - 42A	0.0818%	8.9	**0.324491**	1.849369	-1.20276
Close Valve 6 - 42B	0.0818%	8.9	**0.324491**	1.79696	-1.19946

Close Valve - 36A	0.0818%	8.9	2.857219	1.18564	-0.82154
Close Valve - 36B	0.0818%	8.9	2.857219	1.190932	-0.83144
Close Valve - 30A	0.0818%	8.9	5.040283	0.783328	-0.55535
Close Valve - 30B	0.0818%	8.9	6.361436	0.743091	-0.56577
Close Valve 6 - 42A	0.0818%	31.7	**0.36582**	3.744192	-2.0275
Close Valve 6 - 42B	0.0818%	31.7	**0.387601**	4.304492	-2.30507
Close Valve 6 - 36A	0.0818%	31.7	**2.520263**	2.665712	-1.49551
Close Valve 6 - 36B	0.0818%	31.7	**2.134825**	2.567614	-1.37134
Close Valve 6 - 30A	0.0818%	31.7	2.857219	1.990834	-1.09337
Close Valve 6 - 30B	0.0818%	31.7	2.857219	2.059075	-1.13317
Close Valve 6 - 22B	0.0818%	24.1	3.334704	2.608448	-1.43348
Close Valve 6 - 22C	0.0818%	24.1	3.334704	2.714511	-1.50692
Close Valve 6 - 19A	0.0818%	24.1	4.100943	2.362628	-1.28653
Close Valve 6 - 19B	0.0818%	24.1	4.100943	2.285222	-1.25815
Close Valve 6 - 16A	0.0818%	24.1	5.914396	1.759082	-0.93179
Close Valve 6 - 16B	0.0818%	24.1	5.914396	1.716479	-0.9108
Close Valve 4.75 - 22A	0.0818%	24.1	6.959376	2.729265	-1.49498
Close Valve 4.75 - 22B	0.0818%	24.1	6.959376	2.617796	-1.46071
Close Valve 4.75 - 19A	0.0818%	24.1	8.956927	2.138361	-1.221
Close Valve 4.75 - 19B	0.0818%	24.1	8.956927	2.036834	-1.17454

AIIM SCANNER TEST CHART # 2

Spectra

4 PT ABCDEFGHIJKLMNOPQRSTUVWXYZabcdefghijklmnopqrstuvwxyz:'',./?$0123456789

6 PT ABCDEFGHIJKLMNOPQRSTUVWXYZabcdefghijklmnopqrstuvwxyz;:'',./?$0123456789

8 PT ABCDEFGHIJKLMNOPQRSTUVWXYZabcdefghijklmnopqrstuvwxyz;:'',./?$0123456789

10 PT ABCDEFGHIJKLMNOPQRSTUVWXYZabcdefghijklmnopqrstuvwxyz;:'',./?$0123456789

Times Roman

4 PT ABCDEFGHIJKLMNOPQRSTUVWXYZabcdefghijklmnopqrstuvwxyz;:'',./?$0123456789

6 PT ABCDEFGHIJKLMNOPQRSTUVWXYZabcdefghijklmnopqrstuvwxyz;:'',./?$0123456789

8 PT ABCDEFGHIJKLMNOPQRSTUVWXYZabcdefghijklmnopqrstuvwxyz;:'',./?$0123456789

10 PT ABCDEFGHIJKLMNOPQRSTUVWXYZabcdefghijklmnopqrstuvwxyz;:'',./?$0123456789

Century Schoolbook Bold

4 PT **ABCDEFGHIJKLMNOPQRSTUVWXYZabcdefghijklmnopqrstuvwxyz;:'',./?$0123456789**

6 PT **ABCDEFGHIJKLMNOPQRSTUVWXYZabcdefghijklmnopqrstuvwxyz;:'',./?$0123456789**

8 PT **ABCDEFGHIJKLMNOPQRSTUVWXYZabcdefghijklmnopqrstuvwxyz;:'',./?$0123456789**

10 PT **ABCDEFGHIJKLMNOPQRSTUVWXYZabcdefghijklmnopqrstuvwxyz;:'',./?$0123456789**

News Gothic Bold Reversed

4 PT ABCDEFGHIJKLMNOPQRSTUVWXYZabcdefghijklmnopqrstuvwxyz;:'',./?$0123456789

6 PT ABCDEFGHIJKLMNOPQRSTUVWXYZabcdefghijklmnopqrstuvwxyz;:'',./?$0123456789

8 PT ABCDEFGHIJKLMNOPQRSTUVWXYZabcdefghijklmnopqrstuvwxyz;:'',./?$0123456789

10 PT ABCDEFGHIJKLMNOPQRSTUVWXYZabcdefghijklmnopqrstuvwxyz;:'',./?$0123456789

Bodoni Italic

4 PT ABCDEFGHIJKLMNOPQRSTUVWXYZabcdefghijklmnopqrstuvwxyz;:'',./?$0123456789

6 PT ABCDEFGHIJKLMNOPQRSTUVWXYZabcdefghijklmnopqrstuvwxyz;:'',./?$0123456789

8 PT ABCDEFGHIJKLMNOPQRSTUVWXYZabcdefghijklmnopqrstuvwxyz;:'',./?$0123456789

10 PT ABCDEFGHIJKLMNOPQRSTUVWXYZabcdefghijklmnopqrstuvwxyz;:'',./?$0123456789

Greek and Math Symbols

4 PT ΑΒΓΔΕΞΘΗΙΚΛΜΝΟΠΦΡΣΤΥΩΧΨΖαβγδεξθηικλμνοπφρστυωχψζ≧∓'',. / ≦±=≠°><⊁⊀⩾⩽≡

6 PT ΑΒΓΔΕΞΘΗΙΚΛΜΝΟΠΦΡΣΤΥΩΧΨΖαβγδεξθηικλμνοπφρστυωχψζ≧∓'',. / ≦±=≠°><⊁⊀⩾⩽≡

8 PT ΑΒΓΔΕΞΘΗΙΚΛΜΝΟΠΦΡΣΤΥΩΧΨΖαβγδεξθηικλμνοπφρστυωχψζ≧∓'',. / ≦±=≠°><⊁⊀⩾⩽≡

10 PT ΑΒΓΔΕΞΘΗΙΚΛΜΝΟΠΦΡΣΤΥΩΧΨΖαβγδεξθηικλμνοπφρστυωχψζ≧∓'',. / ≦±=≠°><⊁⊀⩾⩽≡

White

Black

Isolated Characters

e	m	1	2	3	a
4	5	6	7	o	°
8	9	0	h	I	B

A4 Page 6543210

MESH HALFTONE WEDGES

65

85

100

110

133

150

A4 Page 6543210

RIT ALPHANUMERIC RESOLUTION TEST OBJECT, RT-1-71

PRODUCED BY GRAPHIC ARTS RESEARCH CENTER

ROCHESTER INSTITUTE OF TECHNOLOGY, ONE LOMB

MEMORIAL DRIVE, ROCHESTER, NEW YORK 14623